Trade-offs between water loss and carbon gain in a subtropical primary forest on Karst soils in China

Jing Wang[1,2,3]; Xuefa Wen[1,2*], Xinyu Zhang[1,2*], Shenggong Li[1,2]

1 Key Laboratory of Ecosystem Network Observation and Modeling, Institute of Geographic Sciences and Natural Resources Research, Chinese Academy of Sciences, Beijing 100101, China

2 College of Resources and Environment, University of Chinese Academy of Sciences, Beijing 100190, China

3 School of Life Sciences, Beijing Normal University, Beijing 100875, China

*Correspondence: Xuefa Wen (Email: wenxf@igsnrr.ac.cn. Phone +86-010-64889272) and Xinyu Zhang (zhangxy@igsnrr.ac.cn. Phone +86-10-64889679)

Biogeosciences

Discussions

Open Access

EGU

30 **Abstract:**

31 Little attention has been given to plants's trade-off between carbon gain and water

32 loss in Karst Critical Zone in southwestern China with low soil nutrient and water

33 availability. An advanced understanding of the impact of CO_2 diffusion and maximum

34 carboxylase activity of Rubisco (V_{cmax}) on the light-saturated net photosynthesis (A)

35 and intrinsic water use efficiency (iWUE) in Karst plants can provide insight into

36 physiological strategies used in adaptation to harsh environments. We selected six

37 plant life forms (63 species) in a subtropical Karst primary forest in southwestern

38 China, and measured CO_2 response curves, and calculated corresponding stomatal

39 conductance to CO_2 (g_s), mesophyll conductance to CO_2 (g_m), and V_{cmax}. The results

40 showed that g_s varied from 0.05 to 0.38 mol CO_2 m^{-2} s^{-1}, g_m varied from 0.02 to 0.69

41 mol CO_2 m^{-2} s^{-1}, and g_m was positively related to g_s; foliar A was co-limited by g_s, g_m,

42 and V_{cmax} in trees, tree/shrubs, and shrubs with relatively high leaf mass per area

43 (LMA), and mainly constrained by g_m in grasses, vines, and ferns with relatively low

44 LMA; and iWUE varied from 29.52 to 88.92 μmol CO_2 mol^{-1} H_2O across all species,

45 and was significantly correlated with g_s, g_m/g_s, and V_{cmax}/g_s. These results indicated

46 that Karst plants maintained relatively high A and low iWUE through the co-variation

47 of g_s, g_m, and V_{cmax} as adaptation to Karst environment.

48

49 **Key words:** iWUE; mesophyll conductance; stomatal conductance; Karst critical

50 zone; V_{cmax}

Biogeosciences
Discussions

Open Access

EGU

1 Introduction

The Karst Critical Zone (Karst CZ) in southwestern China accounts for over 12% of the total global land area (more than 54×10^4 km^2) (Zhang et al., 2011). Compared with other CZs developed on other lithologies, Karst CZ was developed on limestone bedrock, and characterized by inhomogeneous and shallow soil due to the greater hydraulic erosion and complex underground drainage network (Nie et al., 2014; Chen et al., 2015). In such conditions, the soil cannot retain enough nutrients and water for plant growth even though precipitation is high (1000-2000 mm) (Liu et al., 2011; Fu et al., 2012; Chen et al., 2015). To adapt to the harsh environment, Karst plants develop distinct patterns of light-saturated net photosynthesis (A) and trade-off between carbon gain and water loss to adapt to the harsh environment (Sullivan et al., 2017). The intrinsic water use efficiency (iWUE=A/g_{sw}, the ratio of A to stomatal conductance to H$_2$O (g_{sw})), is an effective indicator of the trade-off between carbon gain and water loss (Moreno-Gutierrez et al., 2012). Until now, variability in A and iWUE has been reported only in 13 co-occurring trees and 12 vines (Chen et al., 2015), and 12 co-occurring tree species (Fu et al., 2012) in two tropical Karst forests in southwestern China.

Based on Fick's first law, A has been shown to be limited only by leaf stomatal conductance to CO$_2$ ($g_s = g_{sw}/1.6$) and V_{cmax} (Flexas et al., 2012; Buckley and Warren, 2014); originally, mesophyll conductance to CO$_2$ (g_m) was proposed to be infinite, i.e. CO$_2$ concentration in chloroplast (C_c) was equal to the CO$_2$ concentration in intercellular air space (C_i). Indeed, g_m varies greatly among species (Warren and Adams, 2006; Flexas et al., 2013). Recent studies have confirmed that A was constrained jointly by g_s, g_m, and V_{cmax}, and their relative contribution to A was species-dependent and site-specific (Carriqui et al., 2015; Tosens et al., 2016; Galmes et al., 2017; Peguero-Pina et al., 2017a; Peguero-Pina et al., 2017b; Veromann-Jurgenson et al., 2017).

Biogeosciences
Discussions

80 Variation in iWUE (=A/g_{sw}) depends on the relative changes in A (g_s, g_m, V_{cmax}) and

81 g_{sw} (g_{sw}=1.6g_s) (Flexas et al., 2013; Gago et al., 2014). Theoretical relationships

82 between iWUE and g_s, g_m, and V_{cmax} have been deduced using two approaches. Based

83 on Fick's first law of CO_2 diffusion, Flexas et al. (2013) deduced that iWUE was a

84 function of g_m/g_s and CO_2 gradients (C_a-C_c) within leaf. On the other hand, combining

85 Fick's first law of CO_2 diffusion and Farquhar biochemical model (Farquhar and

86 Sharkey, 1982), Flexas et al. (2016) deduced that iWUE was a function of V_{cmax}/g_s, C_c,

87 CO_2 compensation point of photosynthesis (Γ^*), and the effective Michaelis–Menten

88 constant of Rubisco for CO_2 (K_m). Until now, most previous studies focused on the

89 role of CO_2 diffusion in limiting iWUE, and suggested that iWUE was negatively

90 related to g_s, and positively related to g_m/g_s (Flexas et al., 2013). Gago et al. (2014)

91 used a meta-analysis with 239 species, and were the first to confirm that iWUE was

92 positively related to V_{cmax}/g_s. Although both g_m/g_s and V_{cmax}/g_s were positively

93 correlated with iWUE, there was only a weak correlation between g_m/g_s and V_{cmax}/g_s,

94 which indicates that iWUE can be improved by increasing V_{cmax} or g_m (proportionally

95 higher than g_s), not both (Gago et al., 2014).

96

97 It is noteworthy that Flexas et al. (2016) and Gago et al. (2014) found that most of the

98 previous work on constraints of g_s, g_m, and V_{cmax} on A were conducted in crops or

99 saplings, and only a few studies were in natural ecosystems. For example, g_m was the

100 main factor limiting A in two Antarctic vascular grasses (Saez et al., 2017), and in 35

101 Australian sclerophylls (Niinemets et al., 2009b) in different habitats. The A of two

102 closely-related Mediterranean *Abies* species growing in two different habitats was

103 mainly constrained by g_m in one, and by g_s in the other habitat (Peguero-Pina et al.,

104 2012). Beyond that, it still remains unknown how g_s, g_m, and V_{cmax} regulate A and

105 iWUE across species in natural ecosystems.

106

107 In this study, we selected 63 dominant plant species, including six life forms (29 trees,

108 11 trees/shrubs, 11 shrubs, 4 grasses, 5 vines, and 3 ferns), from a subtropical primary

109 forest in the Karst CZ of southwestern China, and measured their A and CO_2 response

110   curves. The g_m was calculated using the curve-fitting method (Ethier and Livingston,

111   2004). The obtained g_m was used to transform the A-C_i into A-C_c response curves, and

112   then to calculate the A and V_{cmax}. Our objective was to determine and distinguish the

113   limitations of CO_2 diffusion (g_s and g_m) and V_{cmax} on A and iWUE in different life

114   forms in this Karst primary forest.

115

2 Materials and Methods

2.1 Site information

118   This study was conducted in a subtropical primary forest (26°14′48″N, 105°45′51″E;

119   elevation, 1460 m), located in the Karst CZ of southwestern China. This region has a

120   typical subtropical monsoon climate, with a mean annual precipitation of 1255 mm,

121   and mean annual air temperature of 15.1 ℃ (Zeng et al., 2016). The soils are

122   characterized by a high ratio of exposed rock, shallow and nonhomogeneous soil

123   cover, and complex underground drainage networks, e.g. grooves, channels and

124   depressions (Chen et al., 2010; Zhang et al., 2011; Wen et al., 2016). Soils and soil

125   water are easily leached into underground drainage networks. Soil texture was

126   silt-clay loam, and soil PH was 6.80±0.16 (Chang et al., 2018). The total nitrogen

127   and phosphorus content in soil was 7.30±0.66 and 1.18±0.35 g Kg^{-1}, respectively,

128   which was similar with that of non-Karst CZs (Wang et al., in review). However, the

129   soil quantities (16.04~61.89 Kg m^{-2}) and nitrogen and phosphorus storage (12.04 and

130   1.68 t hm^{-2}) was much lower than that of non-Karst CZs, due to the thin and

131   heterogeneous soil layer (He et al., 2008; Jobbagy et al., 2000; Lu et al., 2010; Li et

132   al., 2008). The typical vegetation type is mixed evergreen and broadleaf deciduous

133   primary forest, dominated by *Itea yunnanensis* Franch, *Carpinus pubescens* Burk*.,*

134   and *Lithocarpus confinis* Huang, etc. (Wang et al., in review).

135

2.2 Leaf gas-exchange measurements

137   In July and August 2016, 63 dominant species of six life forms (Table S1), including

138   29 trees, 11 trees/shrubs, 4 shrubs, 4 grasses, 5 vines, and 3 ferns, were selected for

139   measurements of the A and CO_2 response curves. Details of leaf sampling and

140   measurements of CO_2 response-curves were described in Wang et al. (in review).

141   Briefly, a total of 189 fully sun-exposed, mature leaves were collected from adult

142   individuals of 63 species to measure CO_2 response curves following procedural

143   guidelines (Longand Bernacchi, 2003) using a portable photosynthesis system

144   (Li-6400, Li-Cor, USA).

145

146   A and the corresponding g_{sw} ($g_s=g_{sw}/1.6$), C_a, and C_i were extracted from the CO_2

147   response curve under saturating light (1500 μmol m^{-2} s^{-1}) conditions, with CO_2

148   concentration inside the cuvette set to 400 μmol mol^{-1} (Domingues et al., 2010;

149   Domingues et al., 2010). V_{cmax} was estimated by fitting A-C_c curves (Ethier and

150   Livingston, 2004). The obtained values of g_m were used to transform the A-C_i into

151   A-C_c response curves as $C_c=C_i - A/g_m$.

152

153   The g_m was calculated using a curve-fitting method (Ethier and Livingston, 2004). In

154   this study, calculated C_c and the initial slope of A-C_c curves were above zero,

155   indicating that g_m estimated by the curve fitting method was valid (Warren and

156   Adams, 2006). Further details on the method to calculate g_m are given in Section 4.1.

157

158   **2.3 Theory of trade-off between carbon and water at leaf scale**

159   The exchange of H_2O and CO_2 between the leaf and the atmosphere is regulated by

160   stomata (Gago et al., 2014). According to Fick's first law of diffusion, A and stomatal

161   conductance to CO_2 (g_s) are related as:

162     $$A = g_s(C_a\text{-}C_i) \tag{1}$$

163   where A is the photosynthetic rate (μmol CO_2 m^{-2} s^{-1}); C_a is the ambient CO_2

164   concentration (μmol mol^{-1}); C_i is the intercellular CO_2 concentration (μmol mol^{-1}).

165

166   Besides stomata, mesophyll is another barrier for CO_2 inside the leaf. A and

167   mesophyll conductance to CO_2 (g_m) are related as:

168        $A = g_m(C_i\text{-}C_c)$ (2)

169   where C_c is the CO_2 concentration at the sites of carboxylation (µmol mol^{-1}). C_c not

170   only depends on CO_2 supply by g_m, but also on CO_2 demand (the maximum

171   carboxylase activity of Rubisco, V_{cmax}).

172

173   **(1) The relationship between iWUE and g_m/g_s**

174   iWUE is a function of CO_2 diffusion conductances (e.g. g_s and g_m) and leaf CO_2

175   concentration gradients. We can express A as the product of the total CO_2 diffusion

176   conductance (g_t) from ambient air to chloroplasts, and the corresponding CO_2

177   concentration gradients by combining Eq. (1) and (2) (Flexas et al., 2013):

178        $A = g_t\left[(C_a\text{-}C_i)+(C_i\text{-}C_c)\right]$ (3)

179   where $g_t = 1/(1/g_s+1/g_m)$. This equation demonstrates that CO_2 concentration gradients

180   in leaves are constrained by stomatal and mesophyll resistance to CO_2. Therefore,

181   iWUE can be expressed as：

182        $\dfrac{A}{g_{sw}} = \dfrac{1}{1.6}\ (\dfrac{g_m/g_s}{1+g_m/g_s})\left[(C_a\text{-}C_i)+(C_i\text{-}C_c)\right]$

183   (4)

184   Eq. (4) means that iWUE is positively related to g_m/g_s, but not to g_m itself (Warren

185   and Adams, 2006; Flexas et al., 2013; Buckley and Warren, 2014; Cano et al., 2014).

186

187   **(2) The relationship between iWUE and V_{cmax}/g_s**

188   When Fick's first law and the Farquhar biochemical model (Farquhar and Sharkey,

189   1982) are combined, iWUE is also a function of V_{cmax}. Based on the Farquhar

190   biochemical model (Farquhar and Sharkey, 1982), when A is limited by Rubisco, it

191   can be expressed by the following equation (Sharkey et al., 2007):

192        $A = \dfrac{V_{cmax}(C_c\text{-}\Gamma^*)}{(C_c+K_m)}\text{-}R_d$ (5)

193

194   where Γ^* is the CO_2 compensation point of photosynthesis in the absence of

195   non-photorespiratory respiration in light (R_d), and K_m is the effective

196   Michaelis–Menten constant of Rubisco for CO_2. Combining Eq. (1) and (5) (Flexas et

197   al., 2016), we obtain:

198

$$\frac{V_{\text{cmax}}}{g_{\text{s}}} = \frac{(C_{\text{c}}+K_{\text{m}})(C_{\text{a}}-C_{\text{i}})(A+R_{\text{d}})}{(C_{\text{c}}-\Gamma^{*})A}$$

199 (6)

200 Because R_{d} is much smaller than A in actively photosynthesizing leaves, $V_{\text{cmax}}/g_{\text{s}}$ can

201 be approximated as:

202

$$\frac{V_{\text{cmax}}}{g_{\text{s}}} \approx \frac{(C_{\text{c}}+K_{\text{m}})(C_{\text{a}}-C_{\text{i}})}{(C_{\text{c}}-\Gamma^{*})} = \frac{(C_{\text{c}}+K_{\text{m}})}{(C_{\text{c}}-\Gamma^{*})}\frac{A}{g_{\text{s}}}$$

203 (7)

204 Consequently, iWUE can be expressed as:

205

$$\frac{A}{g_{\text{sw}}} = \frac{1}{1.6}\frac{V_{\text{cmax}}}{g_{\text{s}}}\frac{(C_{\text{c}}-\Gamma^{*})}{(C_{\text{c}}+K_{\text{m}})}$$

206 (8)

207

2.4 Quantitative analysis of limitations on A

209 The relative contribution of g_{s} (l_{s}), g_{m} (l_{m}) and V_{cmax} (l_{b}) to A can be separated by a

210 quantitative limitation model introduced by Jones (Jones, 1985) and further developed

211 by Grassi & Magnani (2005). The sum of l_{s}, l_{m}, and l_{b} is 1. l_{s}, l_{m} and l_{b} can be

212 calculated as:

213

214

$$l_{\text{s}} = \frac{g_{\text{t}}/g_{\text{s}} \cdot \partial A/\partial C_{\text{c}}}{g_{\text{t}}+\partial A/\partial C_{\text{c}}}$$ (12)

215

216

$$l_{\text{m}} = \frac{g_{\text{t}}/g_{\text{m}} \cdot \partial A/\partial C_{\text{c}}}{g_{\text{t}}+\partial A/\partial C_{\text{c}}}$$ (13)

217

218

$$l_{\text{b}} = \frac{g_{\text{t}}}{g_{\text{t}}+\partial A/\partial C_{\text{c}}}$$ (14)

219

220 where $\partial A/\partial C_{\text{c}}$ was calculated as the slope of A-C_{c} response curves over a C_{c} range of

221 50–100 μmol mol^{-1}. l_{s}, l_{m} and l_{b} have no units. A is co-limited by the three factors

222 when $l_{\text{s}}\approx0.3$, $l_{\text{m}}\approx0.3$ and $l_{\text{b}}\approx0.4$ (Galmes, J. et al., 2017).

223

2.5 Statistical analysis

225 The correlation analysis was performed using the least square method, and all of the

226 data were log$_{\text{e}}$-transformed. The probability of significance was defined at p< 0.05.

227

3 Results

3.1 Interrelation among g_s, g_m, g_t, and V_{cmax}

230   CO_2 concentration gradients in leaf were controlled by CO_2 diffusion conductance

231   and V_{cmax}. Fig. 1 shows the relationship between CO_2 gradients (C_a-C_i, C_i-C_c and

232   C_a-C_c) in leaf and the corresponding CO_2 diffusion conductance (g_s, g_m and g_t) (Fig.

233   1a-c), and between C_a-C_c and V_{cmax} (Fig. 1d). CO_2 concentration gradients (C_a-C_i,

234   C_i-C_c and C_a-C_c) were significantly negatively associated with the corresponding CO_2

235   diffusion conductance (g_s, g_m and g_t) ($P<0.001$). V_{cmax} was positively associated with

236   C_a-C_c ($P<0.001$).

237

238   The g_s, g_m, and g_t were significantly positively related to each other ($P<0.001$) (Fig.

239   S1). The contribution of g_m to leaf CO_2 gradient was similar to that of g_s (Fig. S3).

240   The contribution of g_s (57.51–155.13 µmol mol^{-1}) to C_a-C_c (98.50–282.94 µmol mol^{-1})

241   varied from 28% to 86%, and the contribution of g_m (18.15–179.36 µmol mol^{-1}) to

242   C_a-C_c varied from 14% to 72%. But the variation range of g_m (0.02 –0.69 mol CO_2 m^{-2}

243   s^{-1}) was 4.5 times that of g_s (0.05–0.38 mol CO_2 m^{-2} s^{-1}).

244

245   No relationship was found between the CO_2 diffusion conductance (g_s, g_m, and g_t) and

246   V_{cmax} (Fig. S2). However, after normalization of g_s, g_m, g_t, and V_{cmax} for A (normalized

247   parameters are hereafter called $G_S=g_S/A$, $G_m=g_m/A$, $G_t=g_t/A$, and $V=V_{cmax}/A$), V was

248   significantly positively correlated with G_m and G_t ($P<0.001$) (Fig. 2b and c), and was

249   slightly positively correlated with G_s ($P<0.05$) (Fig. 2a), which represented the

250   trade-off between CO_2 supply and demand.

251

3.2 Contribution of g_s, g_m and V_{cmax} to A

253   The variation in A was attributed to variation in both of g_s, g_m, g_t, and V_{cmax}. A was

254   positively correlated with g_s (Fig. 3a), g_m (Fig. 3b), and V_{cmax} (Fig. 3c). We used the

Biogeosciences
Discussions

Open Access

EGU

255 quantitative limitation model (Eqs. (13), (14) and (15)) to separate contributions by g_s

256 (l_s), g_m (l_m), and V_{cmax} (l_b) to limiting A. The l_s, l_m, and l_b were negatively associated

257 with, respectively, g_s, g_m, and V_{cmax} (Fig. 4). The contributions by g_s, g_m, and V_{cmax} to

258 limiting A were different for each species (Fig. S3). l_s varied from 0.17 to 0.45

259 (2.6-fold), l_m varied from 0.05 to 0.55 (10.5-fold), and l_b varied from 0.11 to 0.68

260 (6.2-fold) across species. Overall, g_m contribution to limiting A was the largest

261 ($l_m=0.38\pm0.12$), followed by V_{cmax} ($l_b=0.34\pm0.11$), and g_s ($l_s=0.28\pm0.07$).

262

263 To further understand how A was limited by g_s, g_m, and V_{cmax}, we grouped the 63

264 species into 6 life forms: tree, tree/shrub, shrub, grass, vine, and fern. The averaged

265 leaf mass per area (LMA) of the 6 life forms above were as follows: 69.41 ± 29.31,

266 93.94 ± 27.89, 72.35 ± 42.37, 47.08 ± 16.39, 40.86 ± 13.22 and 44.21 ± 12.35 g m^{-2}.

267 The results showed that tree, tree/shrub, and shrub with relatively high LMA were

268 co-limited by g_s, g_m, and V_{cmax}, while g_m was the main constrain factor for the other

269 three life forms with relatively low LMA (Fig. 5). The l_s showed a decreasing trend

270 from tree to fern. The largest average value of l_s was observed for tree and tree/shrub,

271 followed by shrub, grass, and vine and fern. The l_m first declined, and then increased.

272 Grass had the largest averaged value of l_m. In contrast, l_b first increased and then

273 decreased. Grass had the smallest averaged value of l_b.

274

3.3 Effect of g_s, g_m and V_{cmax} on iWUE

276 The iWUE varied from 29.52 to 88.92 μmol CO_2 mol^{-1} H_2O. In theory, iWUE is

277 regulated by g_s ($g_{sw}=1.6g_s$), g_m, and V_{cmax}. However, a simple correlation analysis

278 showed that iWUE was negatively related to g_s (Fig. 6b), and not related to A (Fig.

279 6a), g_m (Fig. 6c), and V_{cmax} (Fig. 6d).

280

281 A correlation analysis was used to test how g_m/g_s and V_{cmax}/g_s affected iWUE. The

282 results showed that iWUE was positively correlated with g_m/g_s (Fig. 7a) and V_{cmax}/g_s

283 (Fig. 7b). However, there was no significant relationship between g_m/g_s and V_{cmax}/g_s.

284   The iWUE was regulated by co-variation between g_s, g_m and V_{cmax}.

285

4 Discussion

4.1 The role of g_m in CO_2 diffusion and V_{cmax}

288   Three methods are most commonly used for g_m estimation. Those methods have been

289   reviewed by Warren (2006) and Pons et al. (2009). Briefly, g_m can be calculated by

290   the stable isotope method (Evans, 1983; Sharkey et al., 1991; Loreto et al., 1992), J

291   method (Bongi and Loreto, 1989; Dimarco et al., 1990; Harley et al., 1992; Epron et

292   al., 1995; Laisk et al., 2005), and 'curve-fitting' method (Ethier and Livingston, 2004;

293   Sharkey et al., 2007). All of these methods are based on gas exchange measurements

294   (Pons et al., 2009), and some common assumptions (Warren, 2006). Thus, the

295   accuracy of each method is largely unknown (Warren, 2006).

296

297   The g_m was estimated by the 'curve-fitting' method in this study. Although the

298   'curve-fitting' method is less precise than the stable isotope method, the

299   'curve-fitting' method is much more readily available and has been used for several

300   decades (Warren, 2006; Sharkey, 2012). Accurate measurements of A and C_i is a

301   prerequisite for estimating g_m using the 'curve-fitting' method (Pons et al., 2009).

302   Warren (2006) pointed out that highly-accurate measurements need small leaf area

303   and low flow rates. We confirmed that the calculated C_c and the initial slope of A-C_c

304   curves were positive, suggesting that the measured g_m was reliable (Warren, 2006).

305

306   Large variability in g_m has been shown both between and within species with different

307   leaf forms and habits (Gago et al., 2014; Flexas et al., 2016). Variability in g_m in this

308   study is similar to that in global datasets (Gago et al., 2014; Flexas et al., 2016). The

309   order of averaged g_m from different life forms was as follows: tree > tree/shrub >

310   grass > shrub > vine > fern. Previous studies have confirmed that the liquid phase of

311   mesophyll (Veromann-Jurgenson et al., 2017), cell wall thickness of mesophyll

312   (Terashima et al., 2011) or chloroplast (Tosens et al., 2016), and surface area of

Biogeosciences
Discussions

313   mesophyll and chloroplast exposed to intercellular space (Veromann-Jurgenson et al.,

314   2017) were the main limitations for g_m. The LMA varied from 22.98 g m^{-2} to 154.61 g

315   m^{-2}, the averaged value was 69.32±32.70 g m^{-2} (Wang et al., in review). Hence, the

316   wide variability of g_m between different species and life forms in the same ecosystem

317   seems to be related to the diversity in leaf anatomical traits.

318

319   Large uncertainties can be introduced by ignoring g_m. On one hand, g_m plays a similar

320   or somewhat lesser role than g_s in CO_2 diffusion in leaf (Warren, 2006). In the present

321   study, g_m was positively related to g_s (Fig. S1), variability range of g_m was larger than

322   that of g_s, and the contribution of g_m to C_a-C_c was similar to that of g_s. Hence,

323   ignoring g_m would overestimate the carbon isotope discrimination in photosynthesis

324   ($\Delta^{13}C$) (von-Caemmerer, 1996; Warren, 2006). Consistent with previous studies

325   (von-Caemmerer, 1996; Warren, 2006), there was a significantly positive relationship

326   between $\Delta^{13}C\_g_m$ and $\Delta^{13}C\_g_s$ ($\Delta^{13}C\_g_m$=2.38*$\Delta^{13}C\_g_s$-35.54, R^2=0.22, P<0.001).

327    $\Delta^{13}C\_g_m$ represented the carbon isotope discrimination when g_m was finite, and

328    $\Delta^{13}C\_g_s$ represented the carbon isotope discrimination when g_m was infinite.

329

330   On the other hand, ignoring g_m would underestimate V_{cmax} up to 75% (Sun et al.,

331   2014). In this study, the relationship between V_{cmax_Ci} and V_{cmax_Cc} can be expressed as:

332   V_{cmax_Cc}=2.6*V_{cmax_Cc}-22.12 (R^2=0.25, P<0.001). V_{cmax_Ci} represented V_{cmax} calculated

333   based on the A-C_i curve, and V_{cmax_Cc} represented V_{cmax} calculated based on the A-C_c

334   curve. Furthermore, the leaf barrier to CO_2 caused by g_m has not been represented in

335   the global carbon cycles, leading to an overestimation of CO_2 supply for carboxylation

336   and an underestimation of the response of photosynthesis to atmospheric CO_2 (Sun et

337   al., 2014).

338

339   **4.2 Co-variation in g_s, g_m and V_{cmax} in regulating A**

340   The A was constrained by g_s, g_m, and V_{cmax} acting together, however, variability in the

341   relative contribution of these three factors depended on species and habitats (Tosens

342   et al., 2016; Galmes et al., 2017; Peguero-Pina et al., 2017a; Veromann-Jurgenson et

al., 2017). Compared with the global dataset, the A in the study site was high at a given leaf phosphorus (P) level (Wang et al., in review). Under well-watered conditions, A was co-limited by the three factors in angiosperm species (Galmes et al., 2017), and mainly limited by g_m in ferns (Carriqui et al., 2015). Similarly in the present study, A of tree, tree/shrub, and shrub was co-limited by g_s, g_m, and V_{cmax}, and A of fern was mainly limited by g_m. However, A of both grass and vine was mainly limited by g_m (average l_m>0.4, with the largest value of 0.55 and 0.54 for grass and fern, respectively). In addition, 20 of the 63 species were mainly limited by V_{cmax} (l_b>0.4, with the largest value of 0.68).

The importance of g_s and g_m in constraining A was variable, and depended on leaf and mesophyll structural traits, i.e. LMA (Tomas et al., 2013), and thickness of leaf, cell wall (Peguero-Pina et al., 2017b), and mesophyll itself (Giuliani et al., 2013). The negative correlation of g_m with LMA has been reported in previous studies (Niinemets et al., 2009a; Tomas et al., 2013). The lack of correlation between g_m and LMA, and a positive relationship between g_m/LMA and LMA in this study were similar to those shown for gymnosperms (Veromann-Jurgenson et al., 2017). The reason for the similarities may be a strong investment in supportive structures (Veromann-Jurgenson et al., 2017).

A of species with low LMA was co-limited by g_s, g_m, and V_{cmax}, while A of species with high LMA was mainly limited by CO_2 diffusion (Tomas et al., 2013). In this study, trees, tree/shrub, and shrubs with relatively high LMA were co-limited by g_s, g_m, and V_{cmax}, and life forms with low LMA were mainly limited by g_m. Furthermore, we found that g_m was positively related to A (R^2=0.54, P<0.001, Fig. 3b), however, there was no close relationship between g_m and LMA. The reason for this may be that species with high LMA may have thin cell walls in mesophyll (Terashima et al., 2011), and chloroplast (Tosens et al., 2016), or large surface areas of mesophyll and chloroplast exposed to intercellular space (Veromann-Jurgenson et al., 2017); conversely, species with low LMA may have thin cell walls in mesophyll (Terashima

373 et al., 2011), and chloroplast (Tosens et al., 2016), or small surface areas of mesophyll

374 and chloroplast exposed to intercellular space (Veromann-Jurgenson et al., 2017).

375

376 Furthermore, the co-variation of g_s and g_m can also regulate A. Both g_s and g_m are

377 important physical determinants of CO_2 supply from the atmosphere to the

378 chloroplasts (Giuliani et al., 2013). The restricted CO_2 diffusion from the ambient air

379 to chloroplast is the main reason for a decreased A under water stress conditions due

380 to both the stomatal and mesophyll limitations (Olsovska et al., 2016). The

381 relationship between g_s and g_m may reflect a co-variation between A and g_m, or a

382 tendency for g_m to compensate for reductions in g_s (Buckley and Warren, 2014).

383

384 The relative contribution of V_{cmax} to A not only depends on C_a-C_c, but also on leaf

385 nutrient levels. Leaf nitrogen (N) and P were closely related to V_{cmax}. Leaf N:P ratio in

386 the same plants in a related study was 24.55 ± 7.7 (Wang et al., in review), indicating a

387 P limitation to photosynthesis (Gusewell 2004). Although there was no significant

388 relationship between l_m and leaf N:P, there was a trend of increasing l_m with

389 increasing leaf N:P.

390

391 The trade-off between CO_2 supply (g_s and g_m) and demand (carboxylation capacity of

392 Rubisco) can help maintain high photosynthetic efficiency with low CO_2 diffusion

393 conductance (Galmes et al., 2017; Saez et al., 2017). In this study, we used V_{cmax} as a

394 proxy for the carboxylation capacity of Rubisco, and the normalized V_{cmax} by A

395 ($V=V_{cmax}/A$) was significantly negatively correlated with the normalized g_s by A (G_t

396 $=g_s/A$) (P<0.001) (Fig. 2c), indicating that the trade-off between CO_2 supply and

397 demand also existed among different species in the same ecosystems. For genus

398 *Limonium* (flowering plants) (Galmes et al., 2017), g_t was significantly positively

399 related to Rubisco carboxylase specific activity, and significantly negatively related to

400 Rubisco specificity factor to CO_2. In case of Antarctic vascular (Saez et al., 2017) and

401 Mediterranean plants (Flexas et al., 2014), A was mainly limited by low g_m, but it

402 could be partially counterbalanced by a highly-efficient Rubisco through high

Biogeosciences
Discussions
Open Access
EGU

403   specificity for CO_2. This highlights the importance of the trade-off between CO_2

404   supply and demand in plant adaptation to Karst environment. However, it is still

405   unknown how leaf anatomical traits affect g_m and A, and this should be further

406   explored.

407

408   **4.3 Co-variation of g_s, g_m and V_{cmax} in regulating iWUE**

409   Compared with the global dataset under well-watered conditions (19.27-171.88 μmol

410   CO_2 mol^{-1} H_2O) (Flexas et al., 2016), the iWUE (29.52-88.92 μmol CO_2 mol^{-1} H_2O)

411   in this study was somewhat lower in this study. Although Karst soils cannot contain

412   enough water for plant growth, the water use strategies (high g_s/A and low V_{cmax_Ci}/A)

413   were similar to the shown for plants growing in hot and wet regions. Prentice et al.

414   (2014) studied the carbon gain and water loss of woody species in contrasting

415   climates, and found that species in hot and wet regions tend to loss more water in

416   order to fix more carbon (high g_s/A, low V_{cmax_Ci}/A), and vice versa. These results

417   indicates that plants tend to loss more water in order to fix more carbon. However, the

418   variability of iWUE in this study was larger than in the Karst tropical primary forest

419   (Fu et al., 2012; Chen et al., 2015). The average iWUE of 12 vines and 13 trees in the

420   Karst tropical primary forest was 41.23 ± 13.21 μmol CO_2 mol^{-1} H_2O (Chen et al.,

421   2015), while that of 6 evergreen and 6 deciduous trees was 66.7 ± 4.9 and 49.7 ± 2.0

422   μmol CO_2 mol^{-1} H_2O, respectively (Fu et al., 2012)

423

424   The iWUE was regulated by the co-variation of g_s, g_m, and V_{cmax}. In theory, water loss

425   was regulated by g_s only, while A was regulated by g_s, g_m, and V_{cmax} (Fig. 3) (Lawson

426   and and Blatt, 2014). However, iWUE in this study was negatively related to g_s, and

427   not related to A, g_m, or V_{cmax} (Fig. 6). The reason for these relationships maybe that A,

428   g_m, and V_{cmax} co-varied. First, g_s was positively correlated to g_m. Second, an increase

429   in V_{cmax} would inevitably reduce C_c at a given g_s and g_m (Flexas et al., 2016). While

430   no significant relationship was found between V_{cmax} and CO_2 diffusion conductance

431   (g_s, g_m, and g_t), V was negatively correlated with G_s, G_m, and G_t.

Biogeosciences

Discussions

Open Access

EGU

432

433 CO_2 diffusion and Farquhar biochemical model indicated that iWUE was affected by

434 g_m/g_s and V_{cmax}/g_s (Gago et al., 2014; Flexas et al., 2016). There was a hyperbolic

435 dependency of iWUE on g_m/g_s due to the roles of g_s and g_m in C_i and C_c, and of C_c in

436 A (Flexas et al., 2016). In meta-analyses, both Gago et al. (2014) and Flexas et al.

437 (2016) found that iWUE was significantly positively related to g_m/g_s and V_{cmax}/g_s. The

438 results of this study are consistent with the meta-analyses (Fig. 7), demonstrating that

439 plant types with relatively high g_m/g_s or V_{cmax}/g_s had relatively high iWUE.

440

441 However, plants cannot simultaneously have high g_m/g_s and high V_{cmax}/g_s. Similarly to

442 the study of Gago et al. (2014), we found no relationship between g_m/g_s and V_{cmax}/g_s.

443 Gago et al. (2014) thought that the poor relationship between g_m/g_s and V_{cmax}/g_s

444 indicated that the iWUE may be improved by g_m/g_s or V_{cmax}/g_s separately; if both of

445 them were simultaneously improved, the enhanced effect on iWUE could be

446 anticipated. In addition, Flexas et al. (2016) showed in a simulation that the increase

447 in iWUE caused by overinvestment in photosynthetic capacity would progressively

448 lead to inefficiency in trade-off between carbon gain and water use, causing an

449 imbalance between CO_2 supply and demand.

450

451 Water use strategies are critical to the survival and distribution of species, especially

452 in harsh environments, e.g. in low-nutrient availability and water stress (Nie et al.,

453 2014). Species with high g_s, and low iWUE were defined to have

454 'profligate/opportunistic' water use strategy, and species with low g_s and high iWUE

455 were defined to exhibit 'conservative' water use strategy (Moreno-Gutierrez et al.,

456 2012). Species in Karst environment tended to lose more water to gain more carbon,

457 i.e. Karst plants using 'profligate/opportunistic' water use strategy to adapt to the

458 harsh enviroment,.

459

460 **5 Conclusions**

Biogeosciences
Discussions

Open Access

EGU

461 Our results studied the impact factors (g_s, g_m, and V_{cmax}) on A and $iWUE$ in plants with

462 different life forms in field. The different contributions of g_s, g_m, and V_{cmax} to A

463 indicated that plants used diverse trade-off between CO_2 supply and demand to

464 maintain relatively high A. iWUE was relatively low, but ranged widely, indicating

465 that plants used 'profligate/opportunistic' water use strategy to maintain the survival,

466 growth, and structure of the community. Those findings highlight the importance of

467 co-variation of g_s, g_m, and V_{cmax} for the adaptation of plants to the harsh environment.

468 However, the effects of leaf anatomical traits on g_s, g_m, and the trade-off between leaf

469 anatomical traits and V_{cmax} should be further explored.

470

Acknowledgements

474

Author contributions

476 JW, XFW. and XYZ planed and designed the research. JW performed experiments
477 and analyzed data. JW prepared the manuscript with contributions from all
478 co-authors.
479

Competing interests.

481 The authors declare that they have no conflict of interest.

482

6 Reference

484 Bongi, G. and Loreto, F.: Gas-exchange properties of salt-stressed olive (Olea-Europra

485 L) leaves, Plant Physiol., 90, 1408-1416, 1989.

486 Buckley, T.N. and Warren, C.R.: The role of mesophyll conductance in the economics

487 of nitrogen and water use in photosynthesis, Photosynthesis Res., 119, 77-88,

488 2014.

489 Chang, J.J., Zhu, J.X., Xu, L., Su, H.X., Gao, Y., Cai, X.L., Peng, T., Wen, X.F.,

490 Zhang, J.J., He, N.P.: Rational land-use types in the karst regions of China:

491   Insights from soil organic matter composition and stability, Catena, 160, 345-353,

492   2018.

493   Cano, F.J., Lopez, R. and Warren, C.R.: Implications of the mesophyll conductance to

494   CO2 for photosynthesis and water-use efficiency during long-term water stress

495   and recovery in two contrasting Eucalyptus species, Plant Cell Environ., 37,

496   2470-2490, 2014.

497   Carriqui, M., Cabrera, H.M., Conesa, M.A., Coopman, R.E., Douthe, C., Gago, J.,

498   Galle, A., Galmes, J., Ribas-Carbo, M., Tomas, M. and Flexas, J.: Diffusional

499   limitations explain the lower photosynthetic capacity of ferns as compared with

500   angiosperms in a common garden study, Plant Cell Environ., 38, 448-460, 2015.

501   Chen, H., Zhang, W., Wang, K. and Fu, W.: Soil moisture dynamics under different

502   land uses on karst hillslope in northwest Guangxi, China, Environ. Earth Sci., 61,

503   1105-1111, 2010.

504   Chen, P. and Zhou, Y.: Soil nutrient capacity and forest tree sustainability in plateau

505   Karst region. Earth and Enviroment, 45, 32-37, 2017. (In Chinese)

506   Chen, Y.J., Cao, K.F., Schnitzer, S.A., Fan, Z.X., Zhang, J.L. and Bongers, F.:

507   Water-use advantage for lianas over trees in tropical seasonal forests, New

508   Phytol., 205, 128-136, 2015.

509   Dimarco, G., Manes, F., Tricoli, D. and Vitale, E.: Fluorescence Parameters Measured

510   Concurrently with Net Photosynthesis to Investigate Chloroplastic CO_2

511   Concentration in Leaves of Quercus ilex L, J. Plant Physiol., 136, 538-543, 1990.

512   Domingues, T.F., Meir, P., Feldpausch, T.R., Saiz, G., Veenendaal, E.M., Schrodt, F.,

513   Bird, M., Djagbletey, G., Hien, F., Compaore, H., Diallo, A., Grace, J. and Lloyd,

514   J.: Co-limitation of photosynthetic capacity by nitrogen and phosphorus in West

515   Africa woodlands, Plant Cell Environ., 33, 959-980, 2010.

516   Epron, D., Godard, D., Cornic, G. and Genty, B.: Limitation of net CO_2 assimilation

517   rate by internal resistances to CO_2 transfer in the leaves of two tree species

518   (Fagus sylvatica L. and Castanea sativa Mill), Plant Cell Environ., 18, 43-51,

519   1995.

520   Ethier, G.J. and Livingston, N.J.: On the need to incorporate sensitivity to CO_2

521   transfer   conductance   into   the   Farquhar-von   Caemmerer-Berry   leaf
522   photosynthesis model, Plant Cell Environ., 27, 137-153, 2004.

523 Evans, J.R.: Nitrogen and photosynthesis in the flag leaf of Wheat (Triticum aestivum
524   L.), Plant Physiol., 72, 297-302, 1983.

525 Evans, J.R. and Voncaemmerer, S.: Carbon dioxide diffusion inside leaves, Plant
526   Physiol., 110, 339-346, 1996.

527 Farquhar, G.D. and Sharkey, T.D.: Stomatal conductance and photosynthesis, Annu.
528   Rev. Plant Physiol. Plant Mol. Biol., 33, 317-345, 1982.

529 Flanagan, L.B. and Farquhar, G.D.: Variation in the carbon and oxygen isotope
530   composition of plant biomass and its relationship to water-use efficiency at the
531   leaf- and ecosystem-scales in a northern Great Plains grassland, Plant Cell
532   Environ., 37, 425-438, 2014.

533 Flexas, J., Barbour, M.M., Brendel, O., Cabrera, H.M., Carriqui, M., Diaz-Espejo, A.,
534   Douthe, C., Dreyer, E., Ferrio, J.P., Gago, J., Galle, A., Galmes, J., Kodama, N.,
535   Medrano, H., Niinemets, U., Peguero-Pina, J.J., Pou, A., Ribas-Carbo, M.,
536   Tomas, M., Tosens, T. and Warren, C.R.: Mesophyll diffusion conductance to
537   CO_2: An unappreciated central player in photosynthesis, Plant Sci., 193, 70-84,
538   2012.

539 Flexas, J., Niinemets, U., Galle, A., Barbour, M.M., Centritto, M., Diaz-Espejo, A.,
540   Douthe, C., Galmes, J., Ribas-Carbo, M., Rodriguez, P., Rossello, F.,
541   Soolanayakanahally, R., Tomas, M., Wright, I.J., Farquhar, G.D. and Medrano, H.:
542   Diffusional conductances to CO_2 as a target for increasing photosynthesis and
543   photosynthetic water-use efficiency, Photosynthesis Res., 117, 45-59, 2013.

544 Flexas, J., Diaz-Espejo, A., Gago, J., Galle, A., Galmes, J., Gulias, J. and Medrano, H.:
545   Photosynthetic limitations in Mediterranean plants: A review, Environ. Exp. Bot.,
546   103, 12-23, 2014.

547 Flexas, J., Diaz-Espejo, A., Conesa, M.A., Coopman, R.E., Douthe, C., Gago, J.,
548   Galle, A., Galmes, J., Medrano, H., Ribas-Carbo, M., Tomas, M. and Niinemets,
549   U.: Mesophyll conductance to CO_2 and Rubisco as targets for improving intrinsic
550   water use efficiency in C-3 plants, Plant Cell Environ., 39, 965-982, 2016.

551   Fu, P.-L., Jiang, Y.-J., Wang, A.-Y., Brodribb, T.J., Zhang, J.-L., Zhu, S.-D. and Cao,
552   K.-F.: Stem hydraulic traits and leaf water-stress tolerance are co-ordinated with
553   the leaf phenology of angiosperm trees in an Asian tropical dry karst forest, Ann.
554   Bot., 110, 189-199, 2012.

555   Gago, J., Douthe, C., Florez-Sarasa, I., Escalona, J.M., Galmes, J., Fernie, A.R.,
556   Flexas, J. and Medrano, H.: Opportunities for improving leaf water use
557   efficiency under climate change conditions, Plant Sci., 226, 108-119, 2014.

558   Galmes, J., Angel Conesa, M., Manuel Ochogavia, J., Alejandro Perdomo, J., Francis,
559   D.M., Ribas-Carbo, M., Save, R., Flexas, J., Medrano, H. and Cifre, J.:
560   Physiological and morphological adaptations in relation to water use efficiency
561   in Mediterranean accessions of Solanum lycopersicum, Plant Cell Environ., 34,
562   245-260, 2011.

563   Galmes, J., Molins, A., Flexas, J. and Conesa, M.A.: Coordination between leaf CO2
564   diffusion and Rubisco properties allows maximizing photosynthetic efficiency in
565   Limonium species, Plant Cell Environ., 40, 2081-2094, 2017.

566   Giuliani, R., Koteyeva, N., Voznesenskaya, E., Evans, M.A., Cousins, A.B. and
567   Edwards, G.E.: Coordination of leaf photosynthesis, transpiration, and structural
568   traits in rice and wild relatives (Genus Oryza), Plant Physiol., 162, 1632-1651,
569   2013.

570   Grassi, G. and Magnani, F.: Stomatal, mesophyll conductance and biochemical
571   limitations to photosynthesis as affected by drought and leaf ontogeny in ash and
572   oak trees, Plant Cell Environ., 28, 834-849, 2005.

573   Gusewell, S.: N : P ratios in terrestrial plants: variation and functional significance,
574   New Phytol., 164, 243-266, 2004.

575   Harley, P.C., Loreto, F., Dimarco, G. and Sharkey, T.D.: Theoretical considerations
576   when estimating the mesophyll conductance to CO_2 flux by analysis of the
577   response of photosynthesis to CO_2, Plant Physiol., 98, 1429-1436, 1992.

578   He, N.P., Yu, Q., Wu, L., Wang, Y.S. and Han, X.G.: Carbon and nitrogen store and
579   storage potential as affected by land-use in a Leymus chinensis grassland of
580   northern China. Soil Biol. Biochem. 40, 2952-2959, 2008.

581   Jobbagy, E. G. and Jackson, R. B.: The vertical distribution of soil organic carbon and

582   its relation to climate and vegetation. Ecol. Appl. 10, 423-436, 2000.

583   Jones, H.G.: Partitioning stomatal and non-stomatal limitations to photosynthesis,

584   Plant Cell Environ., 8, 95-104, 1985.

585   Laisk, A., Eichelmann, H., Oja, V., Rasulov, B., Padu, E., Bichele, I., Pettai, H. and

586   Kull, O.: Adjustment of leaf photosynthesis to shade in a natural canopy: rate

587   parameters, Plant Cell Environ., 28, 375-388, 2005.

588   Lawson, T. and Blatt, M.R.: Stomatal Size, Speed, and Responsiveness Impact on

589   Photosynthesis and Water Use Efficiency, Plant Physiol., 164, 1556-1570, 2014.

590   Li, Z.P., Han, F. X., Su, Y., Zhang, T.L., Sun, B., Monts, D.L., and Plodinec, M.J.:

591   Assessment of soil organic and carbonate carbon storage in China. Geoderma

592   138, 119-126, 2007.

593   Liu, C.C., Liu, Y.G., Guo, K., Fan, D.Y., Yu, L.F. and Yang, R.: Exploitation of patchy

594   soil water resources by the clonal vine Ficus tikoua in karst habitats of

595   southwestern China, Acta Physiol. Plant., 33, 93-102, 2011.

596   Long, S.P. and Bernacchi, C.J.: Gas exchange measurements, what can they tell us

597   about the underlying limitations to photosynthesis? Procedures and sources of

598   error, J. Exp. Bot., 54, 2393-2401, 2003.

599   Loreto, F., Harley, P.C., Dimarco, G. and Sharkey, T.D.: Estimation of mesophyll

600   conductance to CO_2 flux by three different methods, Plant Physiol., 98,

601   1437-1443, 1992.

602   Lu, X.T., Yin, J.X., Jepsen, M.R. and Tang, J.W.: Ecosystem carbon storage and

603   partitioning in a tropical seasonal forest in Southwestern China. For. Ecol.

604   Manage. 260, 1798-1803, 2010.

605   Moreno-Gutierrez, C., Dawson, T.E., Nicolas, E. and Querejeta, J.I.: Isotopes reveal

606   contrasting water use strategies among coexisting plant species in a

607   Mediterranean ecosystem, New Phytol., 196, 489-496, 2012.

608   Muir, C.D., Conesa, M.A., Roldan, E.J., Molins, A. and Galmes, J.: Weak

609   coordination between leaf structure and function among closely related tomato

610   species, New Phytol., 213, 1642-1653, 2017.

611 Nie, Y.P., Chen, H.S., Wang, K.L. and Ding, Y.L.: Seasonal variations in leaf δ^{13}C

612   values: implications for different water-use strategies among species growing on

613   continuous dolomite outcrops in subtropical China, Acta Physiol. Plant., 36,

614   2571-2579, 2014.

615 Niinemets, U., Diaz-Espejo, A., Flexas, J., Galmes, J. and Warren, C.R.: Role of

616   mesophyll diffusion conductance in constraining potential photosynthetic

617   productivity in the field, J. Exp. Bot., 60, 2249-2270, 2009a.

618 Niinemets, U., Wright, I.J. and Evans, J.R.: Leaf mesophyll diffusion conductance in

619   35 Australian sclerophylls covering a broad range of foliage structural and

620   physiological variation, J. Exp. Bot., 60, 2433-2449, 2009b.

621 Olsovska, K., Kovar, M., Brestic, M., Zivcak, M., Slamka, P. and Shao, H.B.:

622   Genotypically identifying Wheat mesophyll conductance regulation under

623   progressive drought stress, Front. Plant Sci., DOI 10.3389/fpls.2016.01111,

624   2016.

625 Peguero-Pina, J.J., Flexas, J., Galmes, J., Niinemets, U., Sancho-Knapik, D., Barredo,

626   G., Villarroya, D. and Gil-Pelegrin, E.: Leaf anatomical properties in relation to

627   differences in mesophyll conductance to CO_2 and photosynthesis in two related

628   Mediterranean Abies species, Plant Cell Environ., 35, 2121-2129, 2012.

629 Peguero-Pina, J.J., Siso, S., Flexas, J., Galmes, J., Garcia-Nogales, A., Niinemets, U.,

630   Sancho-Knapik, D., Saz, M.A. and Gil-Pelegrin, E.: Cell-level anatomical

631   characteristics explain high mesophyll conductance and photosynthetic capacity

632   in sclerophyllous Mediterranean oaks, New Phytol., 214, 585-596, 2017a.

633 Peguero-Pina, J.J., Siso, S., Flexas, J., Galmes, J., Niinemets, U., Sancho-Knapik, D.

634   and Gil-Pelegrin, E.: Coordinated modifications in mesophyll conductance,

635   photosynthetic potentials and leaf nitrogen contribute to explain the large

636   variation in foliage net assimilation rates across Quercus ilex provenances, Tree

637   Physiol., 37, 1084-1094, 2017b.

638 Perdomo, J.A., Capo-Bauca, S., Carmo-Silva, E. and Galmes, J.: Rubisco and Rubisco

639   Activase Play an Important Role in the Biochemical Limitations of

640   photosynthesis in rice, wheat, and maize under high temperature and water

641   deficit, Front. Plant Sci., DOI: 10.3389/fpls.2017.00490, 2017.

642 Pons, T.L., Flexas, J., Von Caemmerer, S., Evans, J.R., Genty, B., Ribas-Carbo, M.

643   and Brugnoli, E.: Estimating mesophyll conductance to CO_2: methodology,

644   potential errors, and recommendations, J. Exp. Bot., 60, 2217-2234, 2009.

645 Prentice, I.C., Dong, N., Gleason, S.M., Maire, V. and Wright, I.J.: Balancing the

646   costs of carbon gain and water transport: testing a new theoretical framework for

647   plant functional ecology, Ecol. Lett., 17, 82-91, 2014.

648 Saez, P.L., Bravo, L.A., Cavieres, L.A., Vallejos, V., Sanhueza, C., Font-Carrascosa,

649   M., Gil-Pelegrin, E., Peguero-Pina, J.J. and Galmes, J.: Photosynthetic

650   limitations in two Antarctic vascular plants: importance of leaf anatomical traits

651   and Rubisco kinetic parameters, J. Exp. Bot., 68, 2871-2883, 2017.

652 Sharkey, T.D., Vassey, T.L., Vanderveer, P.J. and Vierstra, R.D.: Carbon metabolism

653   enzymes and photosynthesis in transgenic tobacco (Nicotiana tabacum L.)

654   having excess phytochrome, Planta, 185, 287-296, 1991.

655 Sharkey, T.D., Bernacchi, C.J., Farquhar, G.D. and Singsaas, E.L.: Fitting

656   photosynthetic carbon dioxide response curves for C3 leaves, Plant Cell Environ.,

657   30, 1035-1040, 2007.

658 Sharkey, T.D.: Mesophyll conductance: constraint on carbon acquisition by C3 plants,

659   Plant Cell Environ., 35, 1881-1883, 2012.

660 Sun, Y., Gu, L.H., Dickinson, R.E., Pallardy, S.G., Baker, J., Cao, Y.H., Damatta, F.M.,

661   Dong, X.J., Ellsworth, D., Van Goethem, D., Jensen, A.M., Law, B.E., Loos, R.,

662   Martins, S.C.V., Norby, R.J., Warren, J., Weston, D. and Winter, K.:

663   Asymmetrical effects of mesophyll conductance on fundamental photosynthetic

664   parameters and their relationships estimated from leaf gas exchange

665   measurements, Plant Cell Environ., 37, 978-994, 2014.

666 Sullivan, P. L., Wymore, A., McDowell, B., and co-authors: New Opportunities for

667   Critical Zone Science, Report of 2017 Arlington CZO All Hands Meeting

668   white   booklet: Discuss   new   opportunities   for   CZ   Science,

669   http://www.czen.org/sites/default/files/CZO_2017_White_Booklet_20171015a.p

670   df, 2017.

671   Terashima, I., Hanba, Y.T., Tholen, D. and Niinemets, U.: Leaf Functional Anatomy in

672   Relation to Photosynthesis, Plant Physiol., 155, 108-116, 2011.

673   Tomas, M., Flexas, J., Copolovici, L., Galmes, J., Hallik, L., Medrano, H.,

674   Ribas-Carbo, M., Tosens, T., Vislap, V. and Niinemets, U.: Importance of leaf

675   anatomy in determining mesophyll diffusion conductance to CO_2 across species:

676   quantitative limitations and scaling up by models, J. Exp. Bot., 64, 2269-2281,

677   2013.

678   Tosens, T., Nishida, K., Gago, J., Coopman, R.E., Cabrera, H.M., Carriqui, M.,

679   Laanisto, L., Morales, L., Nadal, M., Rojas, R., Talts, E., Tomas, M., Hanba, Y.,

680   Niinemets, U. and Flexas, J.: The photosynthetic capacity in 35 ferns and fern

681   allies: mesophyll CO_2 diffusion as a key trait, New Phytol., 209, 1576-1590,

682   2016.

683   Veromann-Jurgenson, L.L., Tosens, T., Laanisto, L. and Niinemets, U.: Extremely

684   thick cell walls and low mesophyll conductance: welcome to the world of ancient

685   living!, J. Exp. Bot., 68, 1639-1653, 2017.

686   Wang, J., Wen,X.F., Zhang, X.Y., Li, S.G., and Zhang, D.Y.: Magnesium enhances the

687   photosynthetic capacity of a subtropical primary forest in the Karst critical zone.

688   In review.

689   Warren, C.: Estimating the internal conductance to CO_2 movement, Funct. Plant Biol.,

690   33, 431-442, 2006.

691   Warren, C.R. and Adams, M.A.: Internal conductance does not scale with

692   photosynthetic capacity: implications for carbon isotope discrimination and the

693   economics of water and nitrogen use in photosynthesis, Plant Cell Environ., 29,

694   192-201, 2006.

695   Wen, L., Li, D.J., Yang, L.Q., Luo, P., Chen, H., Xiao, K.C., Song, T.Q., Zhang, W.,

696   He, X.Y., Chen, H.S. and Wang, K.L.: Rapid recuperation of soil nitrogen

697   following agricultural abandonment in a karst area, southwest China,

698   Biogeochemistry, 129, 341-354, 2016.

699   Zeng, C., Liu, Z.H., Zhao, M. and Yang, R.: Hydrologically-driven variations in the

700   karst-related carbon sink fluxes: Insights from high-resolution monitoring of

701   three karst catchments in Southwest China, Journal of Hydrology, 533, 74-90,

702   2016.

703 Zhang, X.B., Bai, X.Y. and He, X.B.: Soil creeping in the weathering crust of

704   carbonate rocks and underground soil losses in the karst mountain areas of

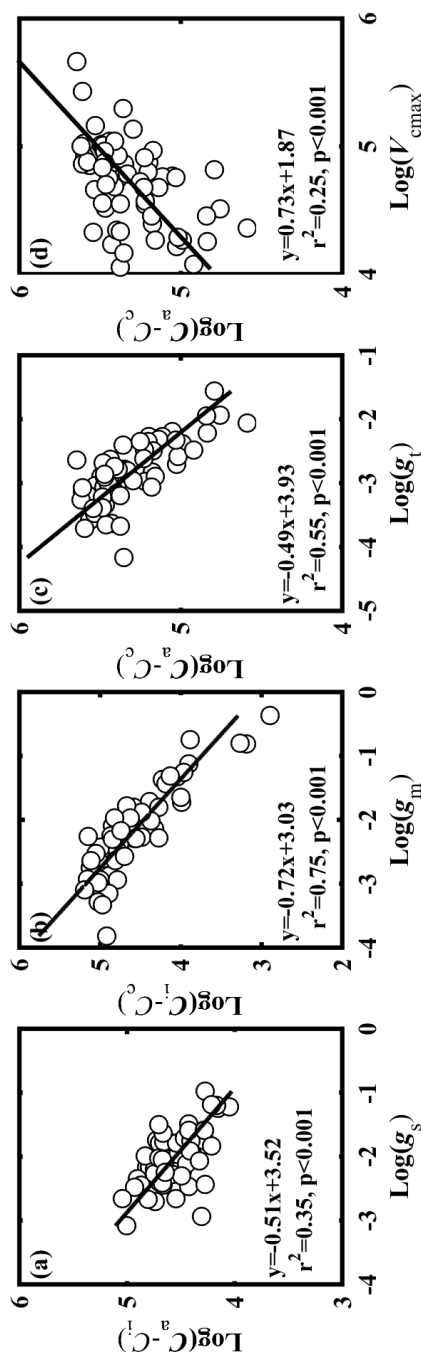705   southwest china, Carbonates and Evaporites, 26, 149-153, 2011.

706

707

708

709

710

711

Figures

Figure 1. Relationships between (a) CO_2 gradient between ambient air and intercellular air space (C_a-C_i, μmol mol^{-1}) and stomatal conductance to CO_2 (g_s, mol CO_2 m^{-2} s^{-1}); (b) CO_2 gradient between intercellular air space and chloroplasts (C_i-C_c, μmol mol^{-1}) and mesophyll conductance to CO_2 (g_m, mol CO_2 m^{-2} s^{-1}); (c) CO_2 concentration gradient between ambient air and chloroplasts (C_a-C_c, μmol mol^{-1}) and total conductance to CO_2 (g_t, mol CO_2 m^{-2} s^{-1}); and (d) C_a-C_c and the maximum carboxylase activity of Rubisco (V_{cmax}, μmol CO_2 m^{-2} s^{-1}).

721

722
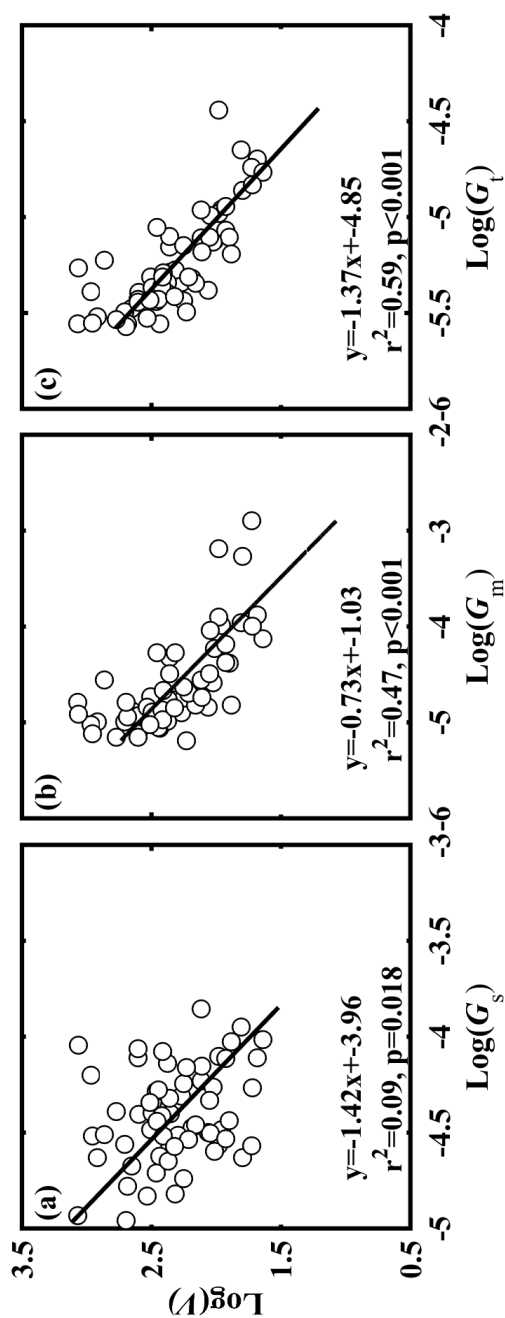
723   Figure 2. Relationships between (a) V and G_s; (b) V and G_m; and (c) V and G_t. V is the ratio of photosynthetic capacity (V_{cmax}) to light-saturated

724   net photosynthesis (A, μmol CO_2 m^{-2} s^{-1}); G_s is the ratio of stomatal conductance to CO_2 (g_s, mol CO_2 m^{-2} s^{-1}) to A; G_m is the ratio of mesophyll

725   conductance to CO_2 (g_m, mol CO_2 m^{-2} s^{-1}) to A; G_t is the ratio of total conductance to CO_2 (g_t, mol CO_2 m^{-2} s^{-1}) to A.

726

727

728
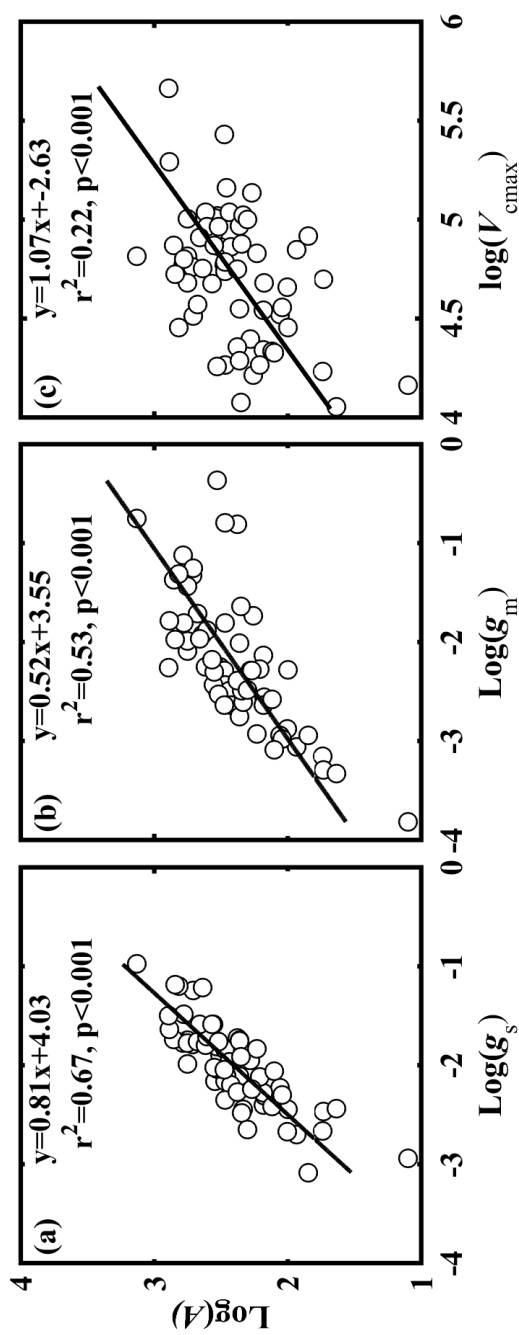
Figure 3. Relationships between light-saturated net photosynthesis (A, µmol CO_2 m^{-2} s^{-1}) and (a) stomatal conductance to CO_2 (g_s, mol CO_2 m^{-2} s^{-1}); (b) mesophyll conductance to CO_2 (g_m, mol CO_2 m^{-2} s^{-1}); and (c) the maximum carboxylase activity of Rubisco (V_{cmax}, µmol CO_2 m^{-2} s^{-1}).

729
730
731
732
733
734
735
736
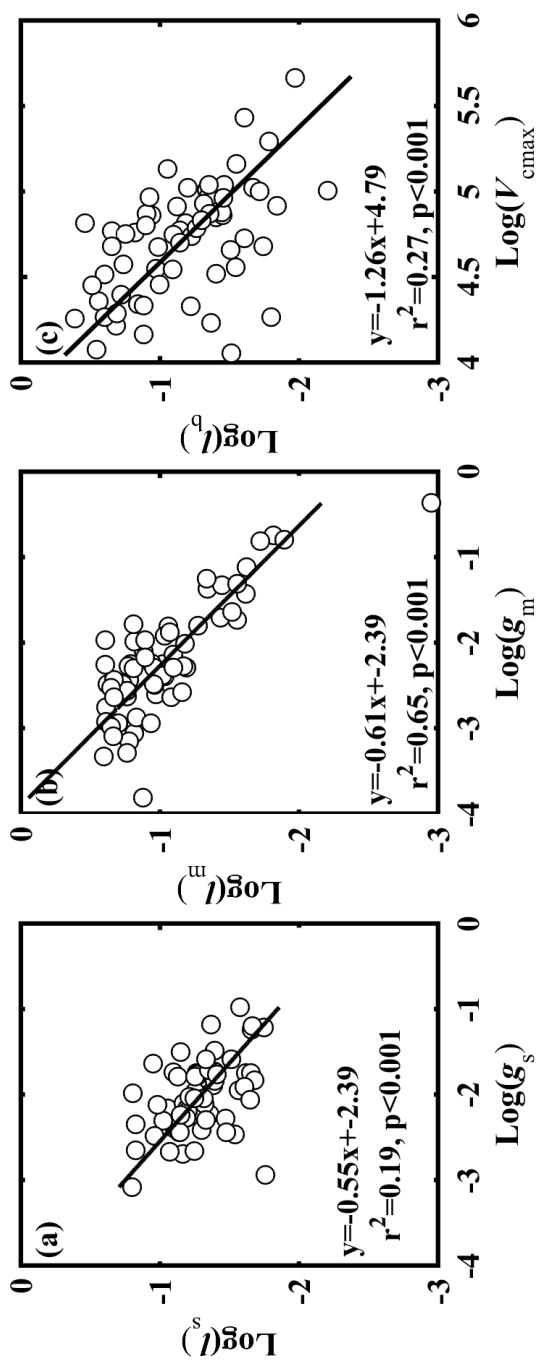
Figure 4. Relationships between (a) stomatal conductance to CO_2 (g_s, mol CO_2 m^{-2} s^{-1}) and l_s (g_s limitation on light-saturated net photosynthesis (A)); (b) mesophyll conductance to CO_2 (g_m, mol CO_2 m^{-2} s^{-1}) and l_m (g_m limitation on A); and (c) the maximum carboxylase activity of Rubisco (V_{cmax}, μmol CO_2 m^{-2} s^{-1}) and l_b (V_{cmax} limitation on A).
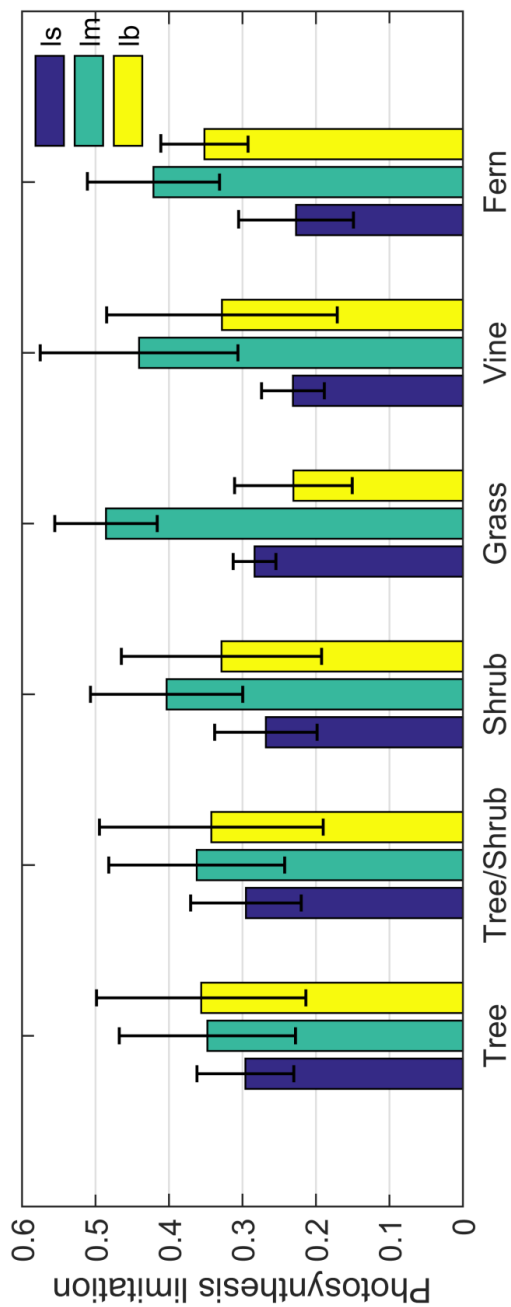
Figure 5. Limitation to light-saturated net photosynthesis (A) in six life forms by stomatal conductance to CO_2 (l_s), mesophyll conductance to CO_2 (l_m), and the maximum carboxylase activity of Rubisco (l_b).
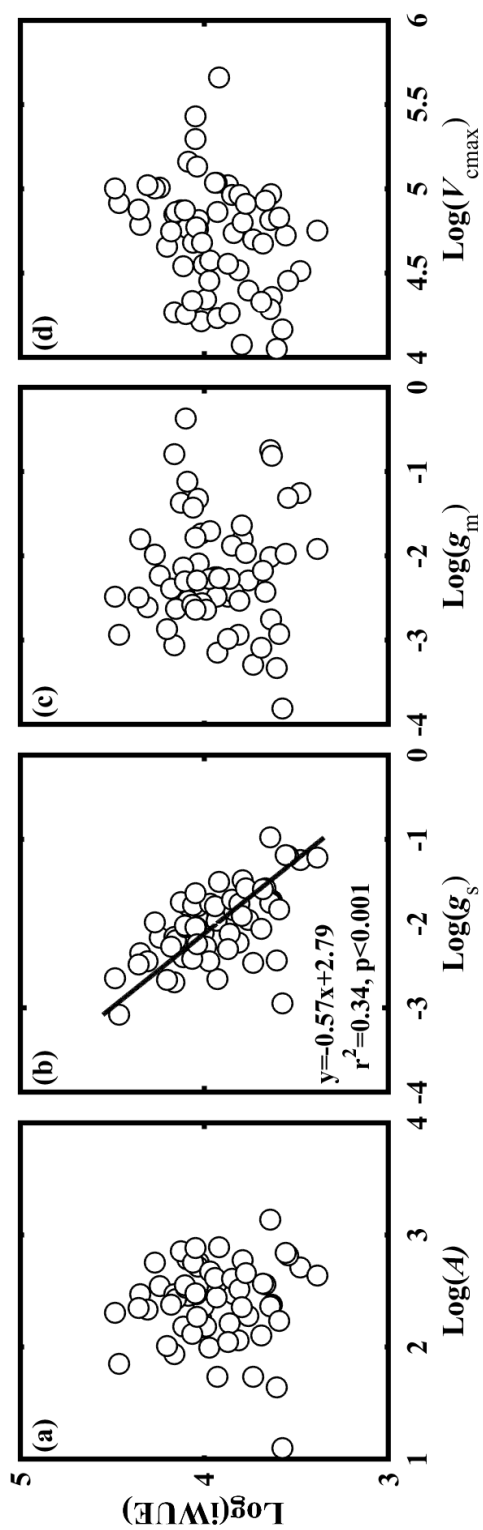
753

754 Figure 6. Relationships between the observed intrinsic water use efficiency (iWUE, μmol CO_2 mol^{-1} H_2O) and (a) light-saturated net

755

756 photosynthesis (A, μmol CO_2 m^{-2} s^{-1}); (b) stomatal conductance to CO_2 (g_s, mol CO_2 m^{-2} s^{-1}); (c) mesophyll conductance to CO_2 (g_m, mol CO_2

757 m^{-2} s^{-1}) and (d) the maximum carboxylase activity of Rubisco (V_{cmax}, μmol CO_2 m^{-2} s^{-1}).

758

759

760

761
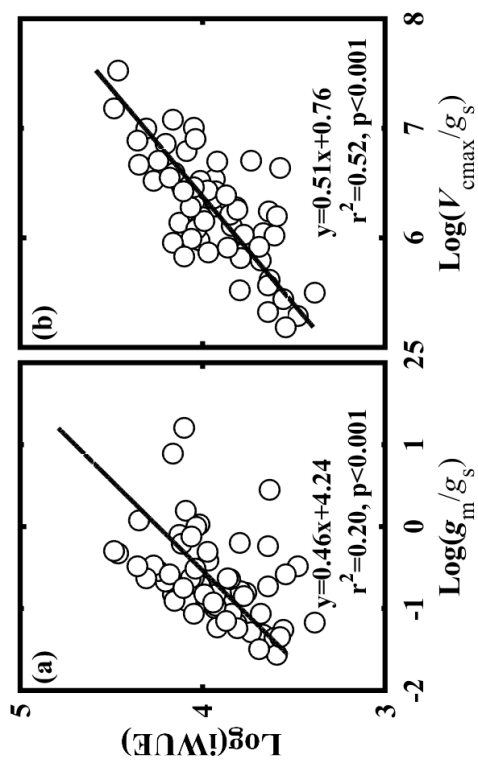
Figure 7. The relationships of the intrinsic water use efficiency (iWUE, μmol CO_2 mol^{-1} H_2O) and (a) the ratio of mesophyll conductance to CO_2

(g_m) to (g_s) (g_m/g_s) and (b) the ratio of the maximum carboxylase activity of Rubisco (V_{cmax}) to gs (V_{cmax}/g_s).